Numerical Simulation of the Pressure Denaturation of a Helical β-Peptide Heptamer Solvated in Methanol

by **Peter J. Gee** and **Wilfred F. van Gunsteren***

Laboratory of Physical Chemistry, Eidgenössische Technische Hochschule, CH-8093 Zurich
(phone: +41-44-632-5501; fax: +41-44-632-1039; e-mail: wfvgn@igc.phys.chem.ethz.ch)

The effect of elevated pressure on the conformational behavior of a β-peptide heptamer (**1**) in MeOH solution was considered. The response of the peptide to elevated pressure was probed by means of molecular dynamics (MD) simulations, and described in atomic terms. The most-striking features of the response are that the region of the 'unfolded' state of the peptide accessible at elevated pressure is narrow, and that thermal and pressure denaturation produce similar 'unfolded' states in the case of **1**.

Introduction. – One way of examining the conformational behavior of a peptidic polymer is to subject it to high pressures both experimentally [1–20] and in computer simulations [21–30]. This is usually done with a view to exploring the 'unfolded state' of large polypeptides such as globular proteins, which remain compact under standard thermodynamic conditions; it is also of interest as a probe of the 'folding–unfolding' behavior of smaller oligopeptides.

In recent years, oligopeptides have been found whose conformational behavior is amenable to study by means of numerical simulations of molecular dynamics (MD) at the atomic level of detail [31–43]. It has been shown that it is now possible to generate a fair representation of the 'folding–unfolding' equilibrium of β-peptides, and this has illustrated that, for such peptides at least, the region of the 'unfolded state', which is accessible under conditions close to the standard thermodynamic state, is much narrower than the full theoretical 'unfolded state' [40] .

The present report seeks to examine the effect of elevated pressure on the conformational behavior of the β-heptapeptide H-β^3-HVal-β^3-HAla-β^3-HLeu-(*S*,*S*)-β^3-HAla(α-Me)-β^3-HVal-β^3-HAla-β^3-HLeu-OH (**1**), whose *Lewis* structure is shown in *Fig. 1*. This peptide has been shown to adopt a 3_1-helical fold under standard conditions [44], and this finding has been reproduced in earlier numerical simulations [31][35]. Data from those earlier reports were used here, and compared with an extra 50-ns MD simulation of the peptide in neat MeOH at 340 K and at an ambient pressure of 1000 atm. A temperature of 340 K has been chosen to approximate the melting temperature of the helix and to maximize the number of (un)folding events of the helix.

The presentation of the simulation results has two concerns. The first is to show the way in which the folding equilibrium at standard pressure changes at high pressure. The second is to illustrate the degree to which the region of the 'unfolded state' accessible at elevated pressure differs from that accessible at elevated temperature with regard to its

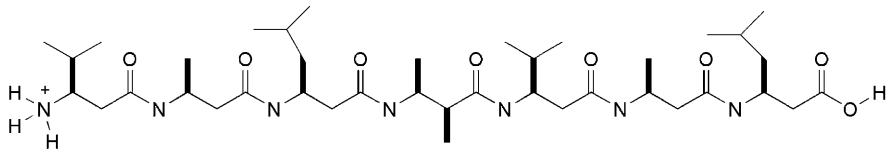

1

Fig. 1. *Formula of the investigated β-peptide heptamer H-β³-HVal-β³-HAla-β³-HLeu-(*S,S*)-β³-HAla-(α-Me)-β³-HVal-β³-HAla-β³-HLeu-OH* (**1**). HVal and HAla refer to homovaline and homoleucine, resp.

breadth and character. Data relevant to these concerns are presented in the *Results* section below, and are remarked upon in the *Discussion*.

Results. – *Proximity to Conformational Equilibrium.* The time course of the number of conformational clusters of each simulation is shown in *Fig. 2*. The number of conformations sampled at 1000 atm is similar to that sampled at 1 atm. Neither curve is rising rapidly, and both simulations may be considered to be close to the conformational equilibrium, at least in so far as this first-order criterion is concerned.

Sampling of the Folded Conformation. In *Fig. 3*, the time-course of the atom-positional root-mean-square deviation (RMSD) of the trajectory structures from the helical NMR model structure using the backbone atoms of residues two to six are shown for both simulations. It is immediately seen that in both runs the NMR-derived helical con-

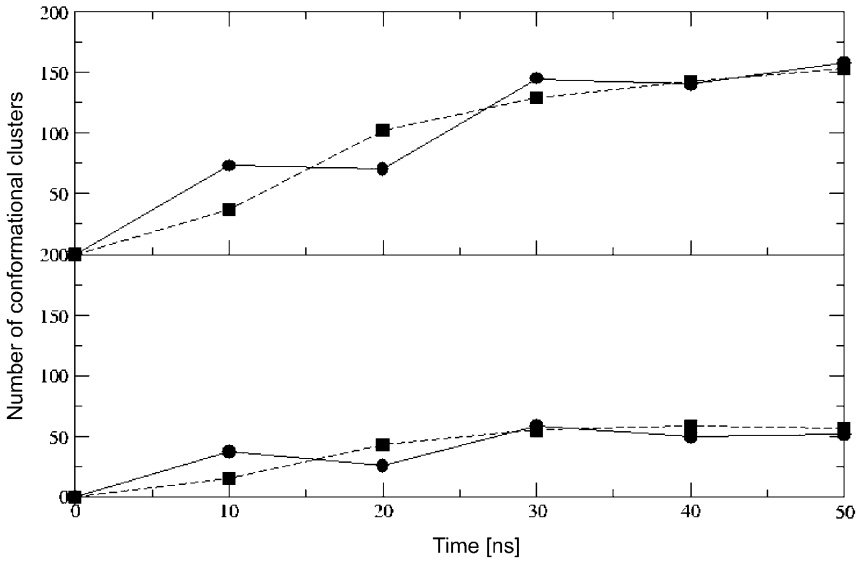

Fig. 2. *Time course of the number of conformational clusters of peptide* **1** *at 340 K and at pressures of 1 atm* (●) *or 1000 atm* (■). Each point in the curves of the upper panel represents the total number of conformational clusters at the corresponding time point. In the lower panel, each point represents the number of conformational clusters that make up 95% of the trajectory sampled at the corresponding time point.

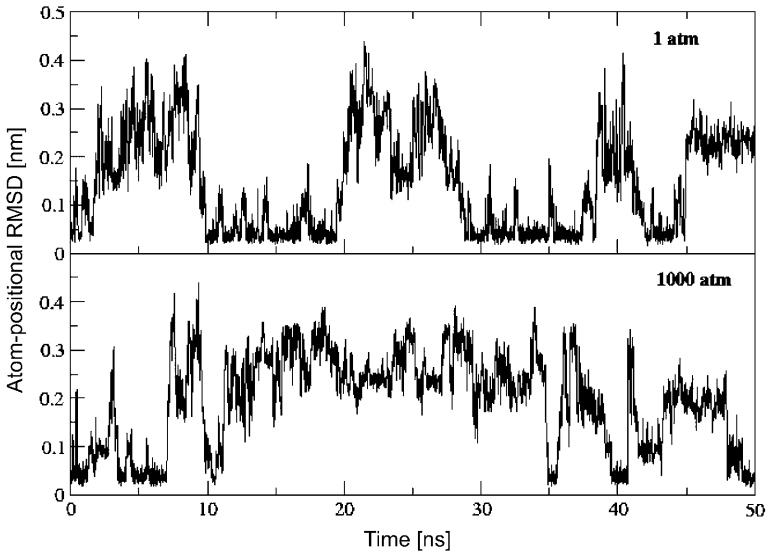

Fig. 3. *Time course of the backbone atom-positional root-mean-square deviation* (RMSD) *from the NMR-derived* 3_1*-helical model conformation of the backbone atoms of internal residues of peptide* **1**. Conditions: at 340 K and a pressure of 1 atm (top) or 1000 atm (bottom).

formation is sampled, and that the degree of sampling seems greater in the run at standard pressure.

Features of the Conformational Distributions. The most-populated conformations in both simulations are summarized in *Fig. 4*. The striking features are *1*) the central-member structure of the first-ranked conformation, which, in both cases, is helix-like, though somewhat more so in the case of the run at 1 atm; and *2*) the relatively small weight (24%) of the first-ranked cluster at 1000 atm, when it is compared with the standard simulation.

Residence in the Folded Conformation. The statistics of residence in the NMR-derived helical conformation are shown in the *Table*. They show more clearly what was seen in *Fig. 3*: at 1000 atm, the peptide spends, overall, less time in the folded conformation and, once it adopts a helical conformation, there is a greater tendency to unfold.

Thermodynamic Characteristics. In the *Table*, estimates of the thermodynamic characteristics of the folding equilibrium of each simulation are shown. As expected, the 'folding–unfolding' equilibrium of the peptide at 1000 atm is shifted to the 'unfolded' side.

Comparison of Unfolded States at Elevated Pressure and Temperature. In *Fig. 5*, the results of a cluster analysis of a trajectory composed of all unfolded configurations of a simulation at elevated temperature (360 K, 1 atm) and of the simulation at 1000 atm (340 K) are shown. (Data for the high-temperature simulation are the same as those presented by *Daura et al.* [35]). It is seen that for almost all conformational clusters characterizing the unfolded state, the number of configurations contributing in the high-temperature simulation is almost equal to the number of configurations contribu-

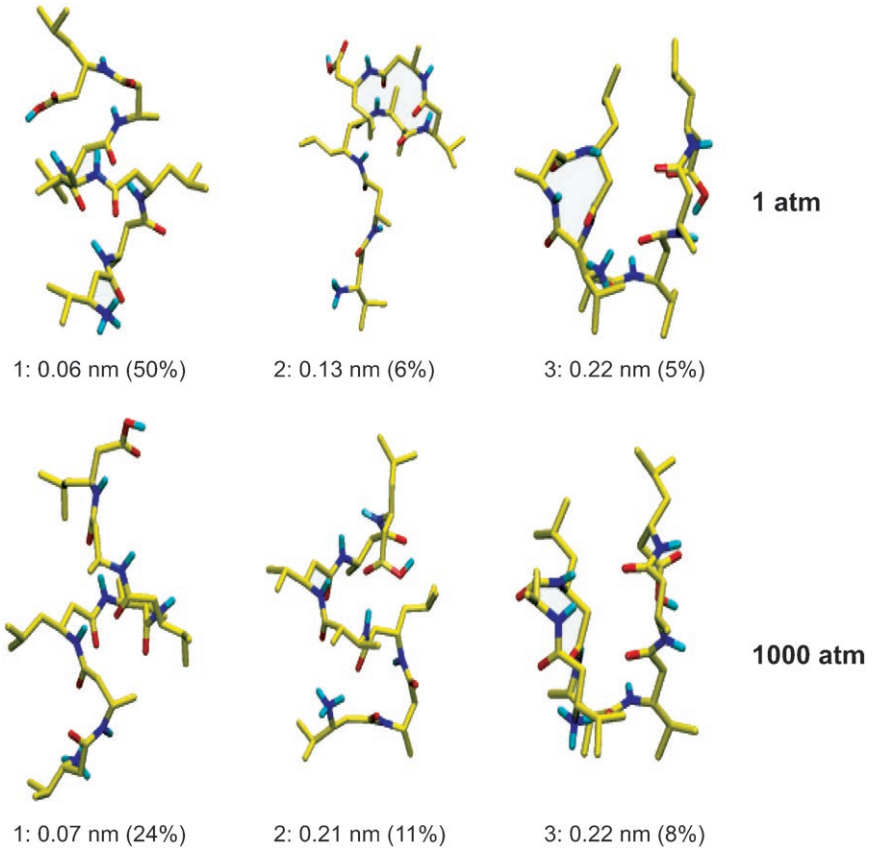

Fig. 4. *Central-member configurations of the three top-ranked or most-populated conformational clusters of peptide* **1**. Conditions: at 340 K and a pressure of 1 atm (upper panel) or 1000 atm (lower panel). The numbers below each configuration show the rank of the conformational cluster represented by the configuration (left); the atom-positional RMSD value from the NMR 3_1-helical model conformation of the backbone atoms of internal residues (middle); and the population (in %) of the trajectory that falls into the cluster represented. In each case, the sample trajectory was 50 ns in length.

ting in the high-pressure simulation. In other words, the conformations characterizing the 'unfolded state' at higher pressure are the same (up to a resolution of 0.1 nm RMSD) as those characterizing the 'unfolded state' at higher temperature.

Discussion. – The results shown above all indicate that peptide **1** becomes denatured at an elevated pressure of 1000 atm. This is most clearly seen in the summary of the conformational distribution shown in *Fig. 4*, where the population of the first-ranked cluster at 1000 atm is much less pronounced than that at standard pressure. Two aspects of the 'unfolded state' at higher pressure are of note: *1*) it is conformationally quite narrow, consisting of *ca*. 150 conformations; *2*) in terms of conformations characterizing this state, it is more or less the same as that sampled at high temperature.

Table. *Thermodynamic and Dynamic Characteristics of the 'Folding–Unfolding' Equilibrium of Peptide* **1** *at Different Pressures.* The margin of error shown derives from an estimate of the folding events as being *Poisson*-distributed. At moderate-to-high intensities, a *Poisson* distribution is approximated by a normal distribution with standard deviation (intensity)$^{1/2}$. Here, the intensity is the number of folding periods, and the margin of error shown is the square root of that number. The change in volume (ΔV) induced by the elevation of pressure is computed as the ratio of the difference in free energy ($\Delta\Delta G$) between the two ensembles and their difference in ambient pressure (ΔP). As the 'folded' state is the same at each pressure, the value of ΔV indicates that the 'unfolded' state is more compact at 1000 atm than it is at 1 atm.

Characteristics	Pressure [atm]	
	1	1000
Number of folding periods	24 ± 5	20 ± 5
Initial residence time [ps]	370	180
Total residence time [ps]	$22\,960 \pm 4822$	$12\,330 \pm 2589$
Mean residence time [ps]	957 ± 201	617 ± 154
Fraction folded	0.46 ± 0.1	0.25 ± 0.1
Equilibrium constant	1.2 ± 0.3	3.1 ± 0.7
Free enthalpy of folding (ΔG) [kJ mol^{-1}]	0.46 ± 0.1	3.16 ± 0.7
$\Delta\Delta G$ [kJ mol^{-1}]	-2.7 ± 0.6	
Difference in pressure (ΔP) [atm]	999	
Volume change (ΔV) on pressure elevation [10^{-24} cm^3]	-44 ± 9	

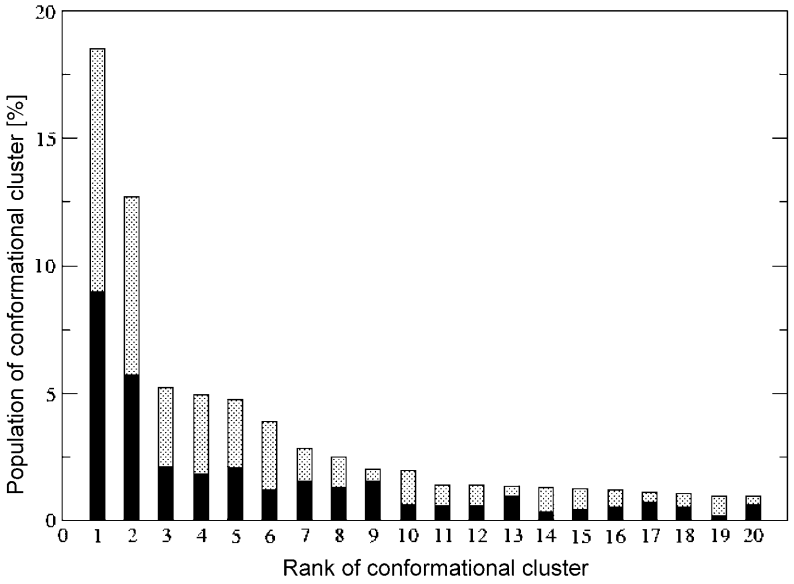

Fig. 5. *Cluster profile of a trajectory containing a simulation of the 'unfolded-state' configurations of peptide* **1**. Conditions: at 360 K and 1 atm (grey); or at 340 K and 1000 atm (black). The 'unfolded state' of each trajectory is defined as the set of all configurations contained in clusters except that of the first rank (most populated, 3_1-helical). Only the first 20 clusters of the combined trajectory are shown.

These findings extend the validity of previous results of *van Gunsteren et al.* [40] as to the narrow extent of the conformational region of the 'unfolded' state of a peptide accessible under standard thermodynamic conditions to non-standard conditions. Since the number of folding events does not increase with increasing pressure, it also shows that studying the (un)folding dynamics at high pressure is not more efficient than at standard pressure.

We thank *Herman J. C. Berendsen* for helpful comments and suggestions. Financial support of the *National Center of Competence in Research* (*NCCR*) *in Structural Biology* by the *Swiss National Science Foundation* (*SNSF*) is gratefully acknowledged.

Experimental Part

Computational Procedure. The data presented in this report are based on two 50-ns MD simulations, one of which (at 1 atm) has been the subject of an earlier report [35]. The simulations were performed with the GROMOS96 package of programs [45][46] and the GROMOS96 43A1 force field [46][47]. Both runs focused on the dynamics of H-β^3-HVal-β^3-HAla-β^3-HLeu-(*S*,*S*)-β^3-HAla(α-Me)-β^3-HVal-β^3-HAla-β^3-HLeu-OH (**1**; *Fig. 1*) in MeOH at 340 K, under an ambient pressure of 1 atm in one case, and under 1000 atm in the other. The molecular models and simulation parameters were those used in [31][48].

Technical specifications of the simulation setup are as follows. Thermodynamic constraints of temperature and pressure were maintained by weak coupling [49] to an external bath. Two thermostats were used: one was coupled to the motion of the solute molecule (**1**), the other to the motion of the solvent molecules (MeOH); both were set with a coupling time of 0.1 ps. The coupling time of the barostat was 0.5 ps, and it was set with an isothermal compressibility of 45.75×10^{-5} (kJ mol^{-1} nm^{-3})$^{-1}$. Forces of interaction were computed in a rectangular simulation cell using periodic boundary conditions and the minimum image convention. Non-bonded interactions were computed with a twin-range cut-off scheme, with radii of 0.8 and 1.4 nm, and the long-range ones were updated every five time steps (each time step being 2 fs). Covalent bonds were kept rigid, with a precision of 10^{-4} using the procedure SHAKE [50].

The initial structure of peptide **1** for both simulations was the 3_1-helical fold. The molecule was surrounded by 962 MeOH molecules in a rectangular box, the dimensions of which were chosen so that the minimum distance from the peptide to the box wall was 1.4 nm in the starting configuration. In both runs, the dimensions of the simulation cell were large enough to accommodate a fully extended conformation of **1**.

Analysis Procedure. The methods and procedure of analysis used to process the simulation data were the same for each run. First, each configuration of the trajectory generated during the simulation was compared to the relevant 'folded' configuration – the helical model structure derived from NMR data. This was done by performing a translational superposition of centers of mass, followed by a least-squares rotational fit to that configuration, and then by computing the atom-positional RMSD value of the backbone atoms of all residues, except the termini. With the definition of a 'folding event' as an interval at the beginning of which the peptide remains 'folded', *i.e.*, with RMSD ≤ 0.1 nm (threshold) for at least 50 ps, and at the end of which it remains unfolded for at least 50 ps, the RMSD time series was then processed to give a distribution of residence times and statistics of that distribution. Estimates of thermodynamic characteristics of the 'folding–unfolding' equilibrium were deduced from these statistics: the equilibrium constant of the folding equilibrium was computed as the ratio of the fraction of time spent unfolded to the fraction of time spent folded; the free energy ΔG was computed as $-RT \ln K$ (where R is the universal gas constant, T the absolute temperature, and K the equilibrium constant); and the volume change on elevation of pressure as the difference in the ΔG of the two state points divided by their difference in pressure. The next stage in the analysis involved comparing, in a similar way to that described above, each configuration in the trajectory to all other configurations in the trajectory. The results of the last step can be pictured as a symmetric square matrix of backbone atom-positional RMSD values. An esti-

mate of the conformational distribution corresponding to the trajectory was constructed from the RMSD matrix using a centroid clustering algorithm [35] that proceeds as follows: a criterion of configurational similarity is set (here 0.1 nm) and used to determine, for each configuration, the number of configurations that are similar to it; the configuration with the largest number of structural neighbors is taken as the center of the first conformational cluster; this configuration and configurations similar to it are then no longer considered; this process is repeated until all configurations are assigned to a cluster. This algorithm generates clusters whose central members have an RMSD value of at least 0.1 nm. It also tends to give many clusters that contain just one member. These are not necessarily conformations that have been sampled once during the run: there may be configurations similar to them that lie just within other clusters.

REFERENCES

[1] C. E. Kundrot, F. M. Richards, *J. Mol. Biol.* **1987**, *193*, 157.
[2] X. D. Peng, J. Jonas, J. L. Silva, *Biochemistry* **1994**, *33*, 8323.
[3] G. J. A Vidugiris, J. L. Markley, C. A. Royer, *Biochemistry* **1995**, *34*, 4909.
[4] K. Goossens, L. Smeller, J. Frank, K. Heremans, *Eur. J. Biochem.* **1996**, *236*, 254.
[5] V. V. Mozhaev, K. Heremans, J. Frank, P. Masson, C. Balny, *Proteins* **1996**, *24*, 81.
[6] G. Panick, R. Malessa, R. Winter, G. Rapp, K. J. Fry, C. A. Royer, *J. Mol. Biol.* **1998**, *275*, 389.
[7] K. Akasaka, H. Li, H. Yamada, R. H. Li, T. Thoresen, C. K. Woodward, *Protein Sci.* **1999**, *8*, 1946.
[8] H. R. Kalbitzer, A. Gorler, H. Li, P. V. Dubovskii, W. Hengstenberg, C. Kowolik, H. Yamada, K. Akasaka. *Protein Sci.* **2000**, *9*, 693.
[9] R. Fourme, R. Kahn, M. Mezouar, E. Girard, C. Hoerentrup, T. Prange, I. Ascone, *J. Synchrotron Radiat.* **2001**, *8*, 1149.
[10] J. L. Silva, D. Foguel, C. A. Royer, *Trends Biochem. Sci.* **2001**, *26*, 612.
[11] C. Balny, P. Masson, K. Heremans, *Biochim. Biophys. Acta – Protein Struct. Mol. Enzym.* **2002**, *1595*, 3.
[12] R. Fourme, I. Ascone, R. Kahn, M. Mezouar, P. Bouvier, E. Girard, T. W. Lin, J. E. Johnson, *Structure* **2002**, *10*, 1409.
[13] J. Jonas, *Biochim. Biophys. Acta – Protein Struct. Mol. Enzym.* **2002**, *1595*, 145.
[14] P. Urayama, G. N. Phillips, S. M. Gruner, *Structure* **2002**, *10*, 51.
[15] M. Refaee, T. Tezuka, K. Akasaka, M. P. Williamson, *J. Mol. Biol.* **2003**, *327*, 857.
[16] Y. O. Kamatari, R. Kitahara, H. Yamada, S. Yokoyama, K. Akasaka, *Methods* **2004**, *34*, 133.
[17] A. Paliwal, D. Asthagiri, D. P. Bossev, M. E. Paulaitis, *Biophys. J.* **2004**, *87*, 3479.
[18] J. Torrent, S. Marchali, P. Tortora, R. Lange, C. Balny, *Cell. Mol. Biol.* **2004**, *50*, 377.
[19] E. Girard, R. Kahn, M. Mezouar, A. C. Dhaussy, T. W. Lin, J. E. Johnson, R. Fourme, *Biophys. J.* **2005**, *88*, 3562.
[20] R. Kitahara, S. Yokoyama, K. Akasaka, *J. Mol. Biol.* **2005**, *347*, 277.
[21] D. B. Kitchen, L. H. Reed, R. M. Levy, *Biochemistry* **1992**, *31*, 10083.
[22] R. M. Brunne, W. F. van Gunsteren, *FEBS Lett.* **1993**, *323*, 215.
[23] P. H. Hünenberger, A. E. Mark, W. F. van Gunsteren, *Proteins* **1995**, *21*, 196.
[24] B. Wroblowski, J. F. Diaz, K. Heremans, Y. Engelborghs, *Proteins* **1996**, *25*, 446.
[25] E. Paci, M. Marchi, *Proc. Natl. Acad. Sci. U.S.A.* **1996**, *93*, 11609.
[26] H. Li, H. Yamada, K. Akasaka, *Biochemistry* **1998**, *37*, 1167.
[27] G. Hummer, S. Garde, A. E. Garcia, M. E. Paulaitis, L. R. Pratt, *Proc. Natl. Acad. Sci. U.S.A.* **1998**, *95*, 1552.
[28] M. Marchi, K. Akasaka, *J. Phys. Chem. B* **2001**, *105*, 711.
[29] E. Paci, *Biochim. Biophys. Acta – Protein Struct. Mol. Enzym.* **2002**, *1595*, 185.
[30] M. Canalia, T. E. Malliavin, *Biopolymers* **2004**, *74*, 377.
[31] X. Daura, B. Jaun, D. Seebach, W. F. van Gunsteren, A. E. Mark, *J. Mol. Biol.* **1998**, *280*, 925.
[32] X. Daura, K. Gademann, B. Jaun, D. Seebach, W. F. van Gunsteren, A. E. Mark, *Angew Chem., Int. Ed.* **1999**, *38*, 236.
[33] M. Takano, T. Yamato, J. Higo, A. Suyama, K. Nagayama, *J. Am. Chem. Soc.* **1999**, *121*, 605.

[34] V. S. Pande, D. S. Rokhsar, *Proc. Natl. Acad. Sci. U.S.A.* **1999**, *96*, 9062.
[35] X. Daura, W. F. van Gunsteren, A. E. Mark, *Proteins: Struct. Funct. Genet.* **1999**, *34*, 269.
[36] B. Y. Ma, R. Nussinov, *J. Mol. Biol.* **2000**, *296*, 1091.
[37] H. W. Wang, S. S. Sung, *J. Am. Chem. Soc.* **2000**, *122*, 1999.
[38] G. Hummer, A. E. Garcia, S. Garde, *Proteins* **2001**, *42*, 77.
[39] X. Daura, K. Gademann, H. Schafer, B. Jaun, D. Seebach, W. F. van Gunsteren, *J. Am. Chem. Soc.* **2001**, *123*, 2393.
[40] W. F. van Gunsteren, R. Bürgi, C. Peter, X. Daura, *Angew. Chem., Int. Ed.* **2001**, *40*, 351.
[41] G. Colombo, D. Roccatano, A. E. Mark, *Proteins* **2002**, *46*, 380.
[42] H. W. Wu, S. M. Wang, B. R. Brooks, *J. Am. Chem. Soc.* **2002**, *124*, 5282.
[43] X. Daura, A. Glättli, P. Gee, C. Peter, W. F. van Gunsteren, *Adv. Protein Chem.* **2002**, *62*, 341.
[44] D. Seebach, P. E. Ciceri, M. Overhand, B. Jaun, D. Rigo, L. Oberer, U. Hommel, R. Amstutz, H. Widmer, *Helv. Chim. Acta* **1996**, *79*, 2043.
[45] W. R. P. Scott, P. H. Hünenberger, I. G. Tironi, A. E. Mark, S. R. Billeter, J. Fennen, A. E. Torda, T. Huber, P. Krüger, W. F. van Gunsteren, *J. Phys. Chem. A* **1999**, *103*, 3596.
[46] W. F. van Gunsteren, S. R. Billeter, A. A. Eising, P. H. Hünenberger, P. Krüger, A. E. Mark, W. R. P. Scott, I. G. Tironi, 'Biomolecular Simulation: The GROMOS96 Manual and User Guide', Vdf Hochschulverlag AG, ETH Zürich, Zürich, 1996.
[47] X. Daura, A. E. Mark, W. F. van Gunsteren, *J. Comput. Chem.* **1998**, *19*, 535.
[48] X. Daura, W. F. van Gunsteren, D. Rigo, B. Jaun, D. Seebach, *Chem.–Eur. J.* **1997**, *3*, 1410.
[49] H. J. C. Berendsen, J. P. M. Postma, W. F. Van Gunsteren, A. DiNola, J. R. Haak, *J. Chem. Phys.* **1984**, *81*, 3684.
[50] J. P. Ryckaert, G. Ciccotti, H. J. C. Berendsen, *J. Comput. Phys.* **1977**, *23*, 327.

Received November 25, 2005